DTU Library

Biochemical and kinetic characterisation of a novel xylooligosaccharide-upregulated GH43 -d-xylosidase/-l-arabinofuranosidase (BXA43) from the probiotic Bifidobacterium animalis subsp. lactis BB-12

Viborg, Alexander Holm; Sørensen, Kim Ib; Gilad, Ofir; Steen-Jensen, Daniel Bisgaard; Dilokpimol, Adiphol; Jacobsen, Susanne; Svensson, Birte

[Link back to DTU Orbit](#)

ORIGINAL ARTICLE

Open Access

Biochemical and kinetic characterisation of a novel xylooligosaccharide-upregulated GH43 β-D-xylosidase/α-L-arabinofuranosidase (BXA43) from the probiotic *Bifidobacterium animalis* subsp. *lactis* BB-12

Alexander Holm Viborg[1], Kim Ib Sørensen[2], Ofir Gilad[1,3], Daniel Bisgaard Steen-Jensen[1], Adiphol Dilokpimol[1], Susanne Jacobsen[1] and Birte Svensson[1*]

Abstract

The *Bifidobacterium animalis* subsp. *lactis* BB-12 gene BIF_00092, assigned to encode a β-D-xylosidase (BXA43) of glycoside hydrolase family 43 (GH43), was cloned with a C-terminal His-tag and expressed in *Escherichia coli*. BXA43 was purified to homogeneity from the cell lysate and found to be a dual-specificity exo-hydrolase active on *para*-nitrophenyl-β-D-xylopyranoside (*p*NPX), *para*-nitrophenyl-α-L-arabinofuranoside (*p*NPA), β-(1 → 4)-xylopyranosyl oligomers (XOS) of degree of polymerisation (DP) 2–4, and birchwood xylan. A phylogenetic tree of the 92 characterised GH43 enzymes displayed five distinct groups (I – V) showing specificity differences. BXA43 belonged to group IV and had an activity ratio for *p*NPA:*p*NPX of 1:25. BXA43 was stable below 40°C and at pH 4.0–8.0 and showed maximum activity at pH 5.5 and 50°C. K_m and k_{cat} for *p*NPX were 15.6 ± 4.2 mM and 60.6 ± 10.8 s^{-1}, respectively, and substrate inhibition became apparent above 18 mM *p*NPX. Similar kinetic parameters and catalytic efficiency values were reported for β-D-xylosidase (XynB3) from *Geobacillus stearothermophilus* T-6 also belonging to group IV. The activity of BXA43 for xylooligosaccharides increased with the size and was 2.3 and 5.6 fold higher, respectively for xylobiose and xylotetraose compared to *p*NPX. BXA43 showed clearly metal inhibition for Zn^{2+} and Ag^+, which is different to its close homologues. Multiple sequence alignment and homology modelling indicated that $Arg^{505}Tyr^{506}$ present in BXA43 are probably important for binding to xylotetraose at subsite +3 and occur only in GH43 from the *Bifidobacterium* genus.

Keywords: Glycoside hydrolase family 43 (GH43); β-D-xylosidase; α-L-arabinofuranosidase; Xylooligosaccharides (XOS); Bifidobacteria; Probiotics

Introduction

Prebiotics are commonly non-digestible oligosaccharides which improve the composition of the gut microbiota thus eliciting beneficial health effects (Macfarlane et al. 2006; van den Broek et al. 2008). With a growing market for prebiotic containing foods there is increasing interest in understanding how prebiotics function at the molecular level. Two approved prebiotics are fructo-oligosaccharides (FOS) and galacto-oligosaccharides (GOS), while β-(1 → 4) linked xylo-oligosaccharides (XOS) with degree of polymerisation (DP) of 2–10 are considered emerging prebiotics (Roberfroid, 2007). Similarly to the approved prebiotics, FOS and GOS, XOS enhance growth of probiotic *Bifidobacterium* and *Lactobacillus* species, while suppressing *Bacteroides species* (Mäkeläinen et al. 2010) and pathogens, *e.g. Clostridium* species (Rycroft et al.

2001). Notably, XOS can lower the amount of secondary bile acids associated with potential tumour-promoting activity (Moure et al. 2006).

XOS are obtained by hydrolysis of xylans, which are linear β-(1 → 4) linked polysaccharides, typically decorated at the 2- and/or 3-position by mono- or di-substitution with α-L-arabinofuranosyl residues and a substitution pattern varying with the botanical origin (Ebringerova 2006). Probiotic bacteria can possess intracellular xylosidases degrading XOS to D-xylose, which in bifidobacteria is metabolised via the D-fructose-6-P shunt, also referred to as the bifid shunt (Ruas-Madiedo et al. 2005). We found a novel β-D-xylosidase BXA43 of glycoside hydrolase family 43 (GH43) (Cantarel et al. 2009) that was highly up-regulated in *Bifidobacterium animalis* subsp. *lactis* BB-12 (BB-12) cultures grown with XOS as the sole carbon source and probably plays an important role in the XOS catabolism (Gilad et al. 2010).

GH43 comprises a broad variety of enzyme specificities (Cantarel et al. 2009) encompassing β-D-xylosidase (EC 3.2.1.37), β-1,3-xylosidase (EC 3.2.1.-), α-L-arabinofuranosidase (EC 3.2.1.55), endo-arabinanase (EC 3.2.1.99), xylanase (EC 3.2.1.8), and galactan 1,3-β-galactosidase (EC 3.2.1.145) of which some are central in biomass utilisation in the biorefinery and bioenergy areas, while others from gut microbiomes of different animals play prominent roles in nutrition and dietary fibre utilisation (Wagschal et al. 2009b; Lagaert et al. 2011; Zhou et al. 2012). Eleven out of the 92 characterised GH43 enzymes are dual-function β-D-xylosidase-α-L-arabinofuranosidases (E.C. 3.2.1.37 / 3.2.1.55) accommodating at subsite −1 D-xylopyranose and L-arabinofuranose residues sharing the spatial orientation of sugar ring hydroxyl groups (Wagschal et al. 2009a). Other enzymes with this dual specificity occur in GH3, 51, and 54 (Jordan et al. 2007; Minic et al. 2004; Shallom et al. 2005; Xiong et al. 2007), however only GH43 uses an inverting mechanism (Armand et al. 1996; Pitson et al. 1996). GH43 and GH62 form clan GH-F (Cantarel et al. 2009) with characteristic 5-fold β-propeller structures available of GH43 β-D-xylosidase, α-L-arabinofuranosidase, arabinanase, and β-1,3-xylosidase (Brüx et al. 2006; Vandermarliere et al. 2009; de Sanctis et al. 2010; Cartmell et al. 2011).

The present study focuses on characterisation of the GH43 β-D-xylosidase/α-L-arabinofuranosidase BXA43 from *Bifidobacterium animalis* subsp. *lactis* BB-12 (BB-12) which was 10–30 fold upregulated in BB-12 grown on XOS as demonstrated by qPCR and DNA microarray analyses (Gilad et al. 2010). This dual-function GH43 was suggested to be important in the catabolism of XOS taken up by BB-12 to D-xylose. A comprehensive phylogenetic analysis of GH43 as well as a homology model provides a basis for the comparative analysis of the enzymatic properties of BXA43.

Materials and methods

Cloning

The BXA43 gene from BB-12 (locus tag BIF_00092, NCBI accession ADC85541), annotated to encode a β-D-xylosidase, was isolated and amplified from chromosomal DNA (provided by Chr. Hansen A/S, Hørshom, Denmark) using upstream primers designed to precede the native Shine-Dalgarno sequence and downstream primers complementary to the 3'-terminus and excluding the stop codon; *Bam*HI and *Xho*I sites are underlined.

Forward: BXA43-5' CGC<u>GGATCC</u>AACCGGGCCGC CGTTTC
Reverse: BXA43-3' CCGC<u>TCGAG</u>TTCACTCAATTC GCGGTAATC

The amplified product was cloned into the pET24(+) expression vector (Novagen) resulting in the plasmid pET24(+)-BXA43 encoding BXA43 with a C-terminal His-tag.

Recombinant expression and purification

Escherichia coli BL21 (DE3) was transformed with pET24(+)-BXA43 and incubated overnight (agar plates, Luria-Bertani (LB), 25 μg/ml kanamycin, 37°C). Transformants were selected based on restriction site patterns and verified by DNA sequencing (Macrogen). A glycerol stock stab of pET24(+)-BXA43 in *E. coli* BL21(DE3) was propagated (20 ml LB medium, 50 μg/ml kanamycin, 37°C overnight) to inoculate LB (500 ml) to $OD_{600} = 0.1$, grown (37°C, 160 rpm) until $OD_{600} = 0.6$ and induced (3 h) by 100 μM isopropyl β-D-1-thiogalactopyranoside. The cells were harvested by centrifugation (3200 g, 20 min) and the pellet stored at −20°C. To purify BXA43 the pellet was resuspended and the cells lysed with 5 ml Bug Buster (Novagen) and 50 U/ml benzonase (Sigma-Aldrich) for 30 min at room temperature, cooled on ice, and centrifuged (as above) to remove debris. The supernatant was filtered (0.45 μm, Millipore), applied to a HisTrap™ HP (1 ml Ni-NTA column, GE Healthcare) equilibrated in 10 mM imidazole, 500 mM NaCl, 30 mM Tris/HCl, pH 8.0 and eluted by a linear gradient of 0–400 mM imidazole in the same buffer. Protein-containing fractions (monitored by A_{280}) were pooled, dialysed against 50 mM Na-acetate pH 5.2 at 4°C overnight (10 kDa cut-off dialysis membrane; Millipore) and concentrated (10 kDa cut-off centrifugal filter; Millipore) to 2.4 mg/ml as determined by aid of amino acid analysis (Barkholt and Jensen 1989). The identity of BXA43 was verified by SDS-PAGE and by peptide mass fingerprinting (Ultraflex II TOF/TOF, Bruker Daltonics) (not shown).

Effect of pH and temperature on stability and activity

The stability of 9.7 nM BXA43 was determined at pH 3–10 by incubation at 4°C for 24 h in Britton-Robinson's universal buffers (Britton and Robinson, 1931) followed by measurement of the residual activity towards *p*NPX (see below). Thermostability of 9.7 nM BXA43 was determined by measuring activity towards *p*NPX after 10 min incubation at 20–65°C in 50 mM Na-acetate, pH 5.2. The temperature dependence of activity towards *p*NPX (see below) was determined in the same range. Half-lives of 9.8 nM BXA43 at 40–60°C were determined in 50 mM Na-acetate, pH 5.2 based on residual activity in aliquots (20 μl) removed at appropriate time intervals, followed by immediate addition of ice-cold 50 mM Na-acetate pH 5.2 (20 μl). Samples were kept on ice until assayed. Half-lives were calculated according to $t_{\frac{1}{2}} = \ln(2) / A e^{-E_a / RT}$, where A is the pre-exponential factor, E_a the activation energy, R the gas constant, and T the temperature in Kelvin.

Enzyme assays

The activity of BXA43 (9.7 nM) towards 1 mM *para*-nitrophenyl-β-D-xylopyranoside (*p*NPX; Sigma) or *para*-nitrophenyl-α-L-arabinofuranoside (*p*NPA; Sigma) was determined from released *para*-nitrophenol measured at 410 nm (ELISA reader; Powerwave XS; Holm & Halby). The substrate in 50 mM Na-acetate, pH 5.2 (40 μl) at 40°C was preincubated (5 min) and the reaction initiated by addition of BXA43 (10 μl) and terminated after 10 min by addition of 1 M Na_2CO_3 (100 μl). One unit was defined as the amount of enzyme (in mg) that releases 1 μmol *para*-nitrophenol/min. Enzymatic activity measurements were performed (in triplicate) according to this procedure, unless otherwise stated.

To determine kinetic parameters, initial rates of hydrolysis were obtained from five time points (0–16 min) and 14 *p*NPX concentrations (0.25–80 mM) using 7.8 nM BXA43 at the above conditions (in duplicates of four independent reactions). Kinetic parameters, k_{cat} (V_{max}), K_m, and K_i were calculated by curve fitting the data to the Michaelis-Menten equation describing substrate inhibition, $v = k_{cat} \times [E] \times S / (K_m + S \times (1 + S/K_i))$, using GraphPad Prism 5 (GraphPad Software).

Activity towards 1% (w/v) birchwood xylan, oat spelt xylan and rye arabinoxylan (all Megazyme) by 78 nM BXA43 was assessed at the above conditions (50 μl) after overnight incubation by thin layer chromatography (TLC; Silica gel 60 F254) of aliquots (1 μl) with arabinose and xylose as reference and developed in 8:2:1 ethylacetate:isopropanol:water for approx. 45 min and dried, followed by staining the carbohydrates with 2% (w/v) orcinol.

The specific activity on 2.25 mM xylobiose (X_2), xylotriose (X_3), and xylotetraose (X_4) (all Megazyme) of

4.9 nM BXA43 was determined in 50 mM Na-acetate pH 5.2 (50 μl), at 40°C for 30 min using the dinitrosalicylic acid (DNS) reducing sugar assay monitored at 540 nm (Miller 1959) with xylose as standard.

The effect of 1 mM Ag^+, Ca^{2+}, Mg^{2+}, Ni^{2+}, or Zn^{2+} on activity towards *p*NPX of 9.8 nM BXA43 was determined essentially as above (in duplicate).
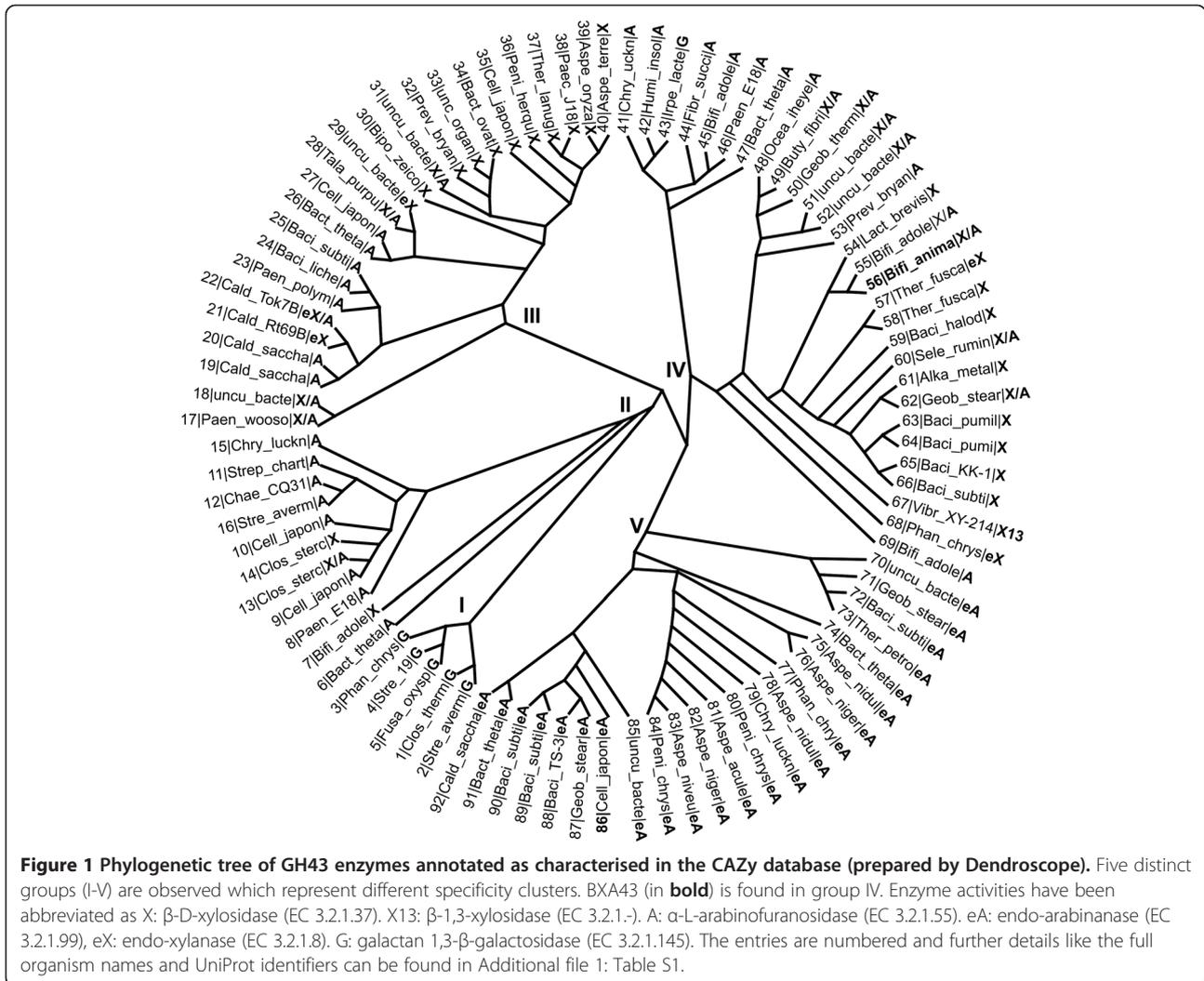
Bioinformatics

Sequences were retrieved of the 92 annotated GH43 enzymes in the CAZy database (Cantarel et al. 2009) and their multiple sequence alignment (ClustalW2; Goujon et al. 2010) was visualised with ESPript (Gouet et al. 1999) and used to construct a phylogenetic tree (Dendroscope; Huson et al. 2007).

A homology model of BXA43 was built (HHPred; Söding et al. 2005) with XynB3 from *Geobacillus stearothermophilus* T-6 (66% similarity, 50% identity; PDB: 2EXH, Brüx et al. 2006) as template. X_4 from the complex with *Bs*AXH-m2,3 from *Bacillus subtilis* subsp. *subtilis* str. 168 (PDB: 3C7G, Vandermarliere et al. 2009) was superimposed at subsites +1 through +4.
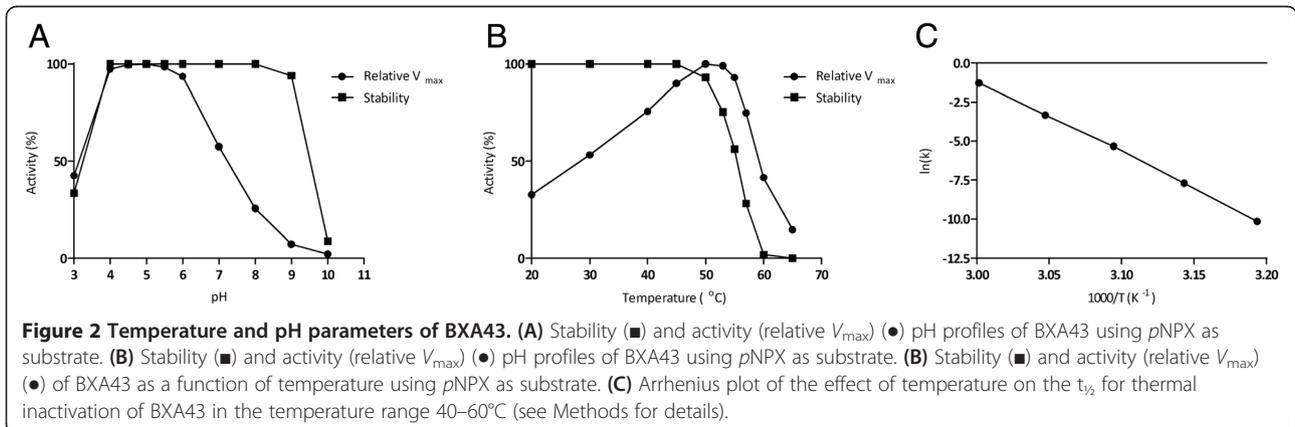
Results

The *BXA43* gene from BB-12, annotated to encode a β-D-xylosidase of GH43 (Cantarel et al. 2009), has an ORF of 1626 nucleotides corresponding to 541 amino acid residues. GH43 (http://www.cazy.org; Cantarel et al. 2009) includes β-D-xylosidases (E.C. 3.2.1.37) and α-L-arabinofuranosidases (E.C. 3.2.1.55) and the phylogenetic tree of 92 GH43 enzymes, which are annotated as characterised in the CAZy database (Cantarel et al. 2009; Figure 1), shows five distinct groups (I – V) representing characteristic substrate specificities. Group I consists of galactan 1,3-β-galactosidases (EC 3.2.1.145), group II mainly of α-L-arabinofuranosidases (EC 3.2.1.55), while group III and IV are divided in two sub-groups, one of which contains predominately extracellular α-L-arabinofuranosidases (EC 3.2.1.55) and the other intracellular β-D-xylosidases (EC 3.2.1.37). Group V is solely composed of endo-arabinanases (EC 3.2.1.99).

Dual-specificity β-D-xylosidase/α-L-arabinofuranosidases are found in GH43 groups II, III, and IV and BXA43 belongs to group IV. The dual specificity β-D-xylosidase/α-L-arabinofuranosidase XylC from *B. adolescentis* ATCC 15703 is the closest well characterised relative (87% similarity, 79% identity; UniProt accession A1A0H6; Lagaert et al. 2011), but BXA43 is also similar to another characterised group IV β-D-xylosidase/α-L-arabinofuranosidase SXA from *Selenomonas ruminantium* GA192 (68% similarity, 52% identity; UniProt accession O52575; Jordan et al. 2007). The crystal structure of a complex with xylobiose (PDB: 2EXH, 2EXJ, Brüx et al. 2006) is available for the group IV β-D-xylosidase XynB3 from *Geobacillus*

Figure 1 Phylogenetic tree of GH43 enzymes annotated as characterised in the CAZy database (prepared by Dendroscope). Five distinct groups (I-V) are observed which represent different specificity clusters. BXA43 (in **bold**) is found in group IV. Enzyme activities have been abbreviated as X: β-D-xylosidase (EC 3.2.1.37). X13: β-1,3-xylosidase (EC 3.2.1.-). A: α-L-arabinofuranosidase (EC 3.2.1.55). eA: endo-arabinanase (EC 3.2.1.99), eX: endo-xylanase (EC 3.2.1.8). G: galactan 1,3-β-galactosidase (EC 3.2.1.145). The entries are numbered and further details like the full organism names and UniProt identifiers can be found in Additional file 1: Table S1.

stearothermophilus T-6 (66% similarity, 50% identity; UniProt accession Q09LX0). A multiple sequence alignment (Additional file 1: Figure S1) shows conservation in BXA43 of the general base and acid catalytic residues Asp[14] and Glu[187] as well as Asp[127] proposed to modulate pK_a of

the catalytic acid (Nurizzo et al. 2002), and various residues involved in substrate binding, including His[250] at subsite –1 (Brüx et al. 2006). It also reveals that BXA43 Tyr[506] and Arg[505], which might be involved in the positioning of Tyr[506], are not conserved in XynB3. These structural

Figure 2 Temperature and pH parameters of BXA43. (A) Stability (■) and activity (relative V_{max}) (●) pH profiles of BXA43 using *p*NPX as substrate. **(B)** Stability (■) and activity (relative V_{max}) (●) pH profiles of BXA43 using *p*NPX as substrate. **(B)** Stability (■) and activity (relative V_{max}) (●) of BXA43 as a function of temperature using *p*NPX as substrate. **(C)** Arrhenius plot of the effect of temperature on the t$_{½}$ for thermal inactivation of BXA43 in the temperature range 40–60°C (see Methods for details).

features may be important for the specificity of BXA43 in particular towards xylooligosaccharides.

Recombinant BXA43 was produced in *E. coli* and purified from the cell lysate in a final yield of 2.2 mg/L culture. It migrated in SDS-PAGE as a single band of approximately 62 kDa in excellent agreement with the theoretical mass of 61,774 Da. BXA43 was stable for 24 h at 4°C at pH 4–9 (Figure 2A). After 10 min at 45°C and 57°C, BXA43 retained 100% and 25% activity, respectively (Figure 2B). The $t_{1/2}$ values of inactivation of 12 d at 40°C, 25.5 h at 45°C, 141 min at 50°C, 19.5 min at 55°C, and 2.5 min at 60°C indicated a linear correlation as described by the Arrhenius equation with activation energy, E_a = 384 kJ/mol (Figure 2C). These data suggest that BXA43 is very stable in the gut, its natural ecological niche.

BXA43 showed maximum activity towards *p*NPX at pH 4.0–5.5 and a temperature optimum of 50°C (Figure 2B). The kinetic parameters as derived from initial rates for hydrolysis of *p*NPX was K_m = 15.6 ± 4.2 mM and k_{cat} = 60.6 ± 10.8 s^{-1} assuming the presence of uncompetitive substrate inhibition with K_i = 29.6 ± 8.5 mM (Figure 3). BXA43 hydrolysed xylooligosaccharides and the specific activity for xylobiose (X_2) was 2.3 fold higher than for *p*NPX and increased further for xylotriose (X_3) and xylotetraose (X_4) (Table 1). The activity towards *p*NPA was 4% of the value for *p*NPX, whereas *para*-nitrophenyl-β-D-galactopyranoside (*p*NPG) was not a substrate (Table 1). TLC indicated release by 20 μM BXA43 of xylose from birchwood xylan, but not from oat spelt xylan or rye arabinoxylan after 24 h incubation. The activity of BXA43 for *p*NPX decreased by 81% in the presence of 1 mM Zn^{2+}, but only by 9% in 1 mM Ag^{+}, while Ca^{2+}, Mg^{2+} or Ni^{2+} did not affect the activity.
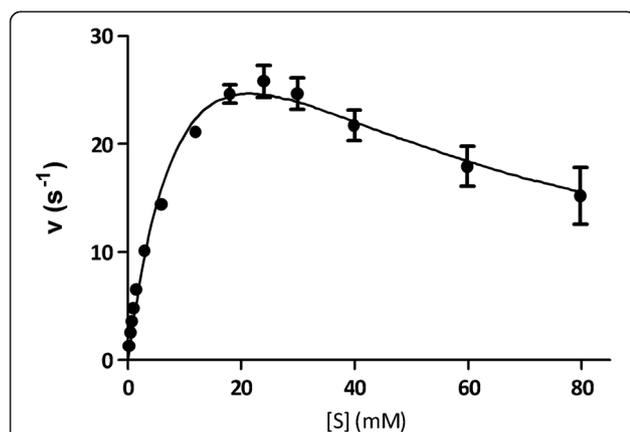

Figure 3 Michaelis-Menten kinetics of BXA43 toward *p*NPX.
The fit is to uncompetitive substrate inhibition. All results are expressed as means ± standard error of the mean (SEM) n = 4 (see Methods for details).

Table 1 Specific activity of BXA43 towards *p*NP-monosaccharides and XOS

Substrate	U/mg
*p*NPX	45.0 (100%)
*p*NPA	1.8 (4%)
*p*NPG	n.d.
Xylobiose (X_2)	105 (233%)
Xylotriose (X_3)	164 (364%)
Xylotetraose (X_4)	253 (562%)

n.d. not detected.

Discussion

BXA43 of *Bifidobacterium animalis* subsp. *lactis* BB-12 from GH43 was produced recombinantly in *E. coli* BL21 (DE3) and showed K_m of 15.6 ± 4.6 mM, k_{cat} of 60.6 ± 10.8 s^{-1} and the catalytic efficiency k_{cat}/K_m of 3.9 s^{-1} mM^{-1} similar to k_{cat} of 57 s^{-1} and k_{cat}/K_m of 3.3 s^{-1} mM^{-1} reported for β-xylosidase (XynB3) from *Geobacillus stearothermophilus* T-6 (Brüx et al. 2006). By contrast, β-xylosidase/α-L-arabinofuranosidase from *S. ruminantium* GA192 has much lower K_m = 0.38 mM (Brunzelle et al. 2008), and a β-xylosidase from *Bacillus pumilus* IPS has K_m = 3.9 mM (Xu et al. 1991). Remarkably, V_{max} of BXA43 of 166 U mg^{-1} was 11-fold higher than V_{max} of 15 U mg^{-1} obtained for the GH43 enzyme from the thermophile *Clostridium stercorarium* F-9 (Suryani et al. 2004). BXA43 showed decreased rate of hydrolysis above 18 mM *p*NPX indicating apparent substrate inhibition (K_i = 29.6 ± 8.5 mM), which however, was not a result of product condensation as verified by TLC (data not shown) consistent with no reports of condensation activity of GH43 enzymes. By contrast, the retaining *Thermoanaerobacter ethanolicus* β-xylosidase/α-L-arabinofuranosidase from GH3 was subject to substrate inhibition at low substrate concentration of 0.5 mM *p*NPX (Mai et al. 2000).

As BXA43 has 5°C lower temperature optimum than the group IV enzyme deXA isolated from a compost starter mixture (Wagschal et al. 2009a) the thermal half-lives determined of BXA43 (141 min at 50°C; 19.5 min at 55°C; 2.5 min at 60°C) and deXA (630 min at 49°C; 234 min at 51°C; 47 min at 53°C) are comparable. BXA43 was inhibited by 1 mM Zn^{2+} and less sensitive to Ag^{+}, while a GH43 β-D-xylosidase from *Talaromyces thermophilus* was inhibited by both Zn^{2+}, Cu^{2+} and Hg^{2+} (Guerfali et al. 2008). Remarkably, 1 mM Zn^{2+} had no effect on activity of the β-D-xylosidase/α-L-arabinofuranosidase from *G. stearothermophilus* T-6, which has 66% sequence identity and similar specific activity to BXA43, whereas 1 mM Ag^{+} inactivated this enzyme (Shallom et al. 2005). Thus, distinctly different metal ion sensitivity is observed among GH43 enzymes.

BXA43 hydrolysed X_2, X_3, and X_4 in line with a suggested model for XOS utilisation in BB-12 that includes uptake *via* an ATP binding cassette (ABC) oligosaccharide transport system whose components were identified in the secreted (secretome) and the membrane proteomes of BB-12 grown on XOS; BB-12 is incapable of growing on xylose as the sole carbon source (Gilad et al. 2011; 2012). While an increasing specific activity for X_2, X_3, and X_4 (Table 1) is seen for BXA43, this was not reported for GbtXyl43A from *G. thermoleovorans* IT-08 (Wagschal et al. 2009b) and deAX from an uncultured bacterium (Wagschal et al. 2009a) which both belong to group IV and have the highest specific activity on X_2 or X_3, respectively. This can possibly be explained by the uniqueness of the BXA43 Tyr^{506} residue, found only within the *Bifidobacterium* and *Lactobacillus* GH43 enzymes. This residue may stack onto substrate at subsite +3 in BXA43, as supported by homology modelling (Figure 4). Interestingly, the group IV XylC from *B. adolescentis* ATCC 15703 that is hypothesised to play an important role in the efficient conversion of X_2 to xylose (Lagaert et al. 2011), possesses the corresponding tyrosine residue, has slightly higher specific activity on X_2 (23.7 s^{-1} mM^{-1}) than X_4 (17.0 s^{-1} mM^{-1}), and the highest specific activity observed towards xylohexaose (X_6, 24.6 s^{-1} mM^{-1}). Notably, *B. adolescentis* ATCC 15703 also harbours a GH120 β-D-xylosidase (XylB), not found in BB-12, which shows a drastic increase in specific activity from X_2 (0.7 s^{-1} mM^{-1}) to X_4 (17.6 s^{-1} mM^{-1}, Lagaert et al. 2011).

A phylogenetic tree (Figure 1) generated for characterised GH43 enzymes, as annotated by the CAZy database (Cantarel et al. 2009) of which approximately 35% have been studied and 13 have a known *p*NPX:*p*NPA activity ratio (Table 2), has five clusters (groups I – V) (Figure 1) representing distinct substrate specificities, as opposed to a previously reported phylogenetic tree (Qian et al. 2003) that displayed four groups. The two phylogenetic trees, however, are based on different dataset and are analysed with different purposes, therefore their group numbering is not directly comparable. The newly updated tree provides more
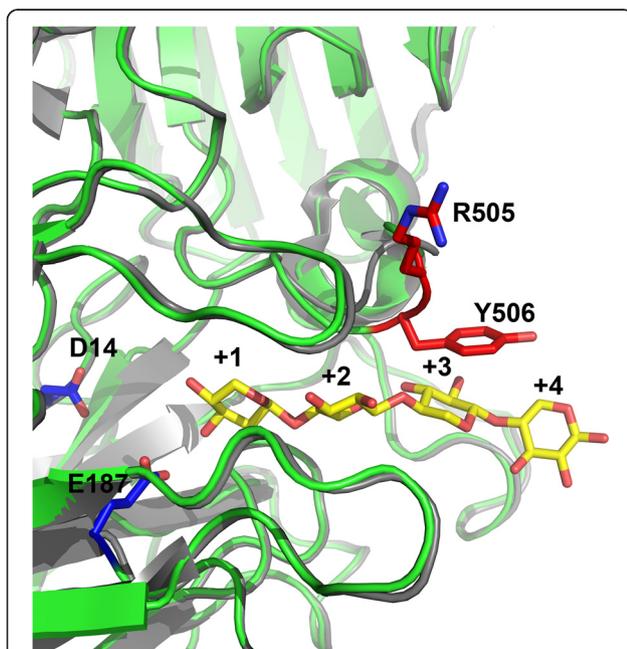

Figure 4 Model of BXA43 (green) superimposed with the structure of the close homolog XynB3 (grey, 2EXH), showing the two catalytic residues D^{14} and E^{187} (in blue; BXA43 numbering). Xylotetraose (yellow) was manually fitted from the structure of the complex with *Bs*AXH-m2,3 on *Bacillus subtilis* (grey, 3C7G) (Vandermarliere *et al.,* 2009) occupying the +1, +2, +3, and +4 subsites and illustrating a predicted +3 subsite involvement of Y^{506} (red). Arg^{505} in BXA43 may play a role in the positioning of Tyr^{506}.

Table 2 *p*NPX: *p*NPA activity ratio of biochemically characterised dual-function β-D-xylosidases/α-L-arabinofuranosidases from GH43

Enzyme name Organism (UniProt identifier)	*p*NPX: *p*NPA ratio	Phylogenetic group[a]	Reference
C. stercorarium (P48790)	2.5	II	Sakka et al. 1993
RunXyn1 Uncultured rumen bacterium (E3TBJ3)	2.6	III	Zhou et al. 2012
r_09-02 uncultured bacterium r_09 (I6YTF5)	1.1	III	Ferrer et al. 2012
XylC *Paenibacillus woosongensis* (E7DXB6)	1.9	III	Kim and Yoon 2010
ABF3 *P. purpurogenum* (C3W4Y2)	5.2	III	Ravanal et al. 2010
BXA43 *B. animalis* subsp. *lactis* BB-12 (D3R467)	25.0	IV	This study
XynB3 *G. stearothermophilus* T-6 (Q09LX0)	22.2	IV	Shallom et al. 2005
SXA *S. ruminantium* GA192 (O52575)	12.7	IV	Whitehead and Cotta, 2001
XylC *B. adolescentis* ATCC 15703 (A1A0H6)	9.1	IV	Lagaert et al. 2011
XylB *B. fibrisolvens* GS 113 (P45982)	0.6	IV	Utt et al. 1991
deAFc Uncultured bacterium (A0S5D8)	0.6	IV	Wagschal et al. 2007
deAX Uncultured bacterium (B8QP77)	0.5	IV	Wagschal et al. 2009a
GbtXyl43A *G. thermoleovorans* IT-08 (Q2I2N4)	0.1	IV	Wagschal et al. 2009b

[a]This study.

specific grouping, most likely due to the better current annotation of the GH43 genes, as biochemical data have been reported for all proposed five phylogenetic groups after the previous tree was published.

BXA43 is classified as a dual-function β-xylosidase/α-L-arabinofuranosidase of group IV (Figure 1). Dual-function β-xylosidases/α-L-arabinofuranosidases occur in groups II, III and IV and their pNPX:pNPA activity ratios vary in the range 0.1–25 (Table 2), with BXA43 having highest and almost the same ratio as XynB3 from *G. stearothermophilus* T-6 (Shallom et al. 2005). The relatively low activity of BXA43 for pNPA suggests, as previously hypothesised (Gilad et al. 2010), a main role of BXA43 in intracellular hydrolysis of XOS. BLASTP searches revealed that only enzymes of the *Bifidobacterium* genus contain both Arg[505] and Tyr[506] proposed to be implicated in high activity on xylooligosaccharides. One gene, however, from *Lactobacillus brevis* ATCC 367 (ABJ65333.1, Makarova et al. 2006) from group IV, is annotated as β-xylosidase and encodes a tyrosine in the same position as Tyr[506], but the corresponding protein has not been described.

BXA43 was able to release xylose from birchwood xylan, but not from oat spelt xylan or rye arabinoxylan. While arabinose substituents increase the bulkiness of xylans and can interfere with their accommodation in the active site of enzymes from GH43, it appears that α-(1 → 2)-4-*O*-methyl-D-glucuronic acid substituents on birchwood xylan are oriented in a way that allows BXA43 to hydrolyse the release of a xylosyl residue preceding to a substituted backbone xylosyl residue (Tenkanen et al. 1996). Arabinose was not detected after incubation of oat and rye arabinoxylans with BXA43, thus the active site seemed unable to accommodate arabinose substituents of these polysaccharides in a productive manner at subsite −1 despite its clear activity on pNPA. A similar observation is reported for XylC from *B. adolescentis* ATCC 15703 (Lagaert et al. 2011). However without structural data on these enzymes and their interaction with *e.g.* xylotetraose at the active site it is not readily explained why they do not release arabinose from oat and rye arabinoxylans.

Additional file

Additional file 1: Figure S1. Multiple sequence alignment using ESPript (Gouet et al. 1999) of GH43 phylogenetic group IV, including BXA43 (ADC85541.1) and XynB3 (AAT98625.1), reveals that BXA43 R[505] and Y[506] (red stars), which are located in the spatial proximity of the active site, are not conserved in XynB3. BAF39209.1 from *Bifidobacterium adolescentis* ATCC 15703 illustrates the conserved R[505] and Y[506] in Bifidobacteria. Catalytic residues (green stars) and the proposed histidine (Brüx et al. 2006) involved in subsite −1 interaction (blue star). **Table S1.** Organisms associated with GenBank accessions in Figure 1.

Competing interests

The authors declare that they have no competing interests.

Author details

[1]Enzyme and Protein Chemistry, Department of Systems Biology, Technical University of Denmark, Søltofts Plads, Building 224, DK-2800 Kgs, Lyngby, Denmark. [2]Department for Strains, Chr. Hansen A/S, 2970 Hørsholm, Denmark. [3]Department for Identification, Chr. Hansen A/S, 2970 Hørsholm, Denmark.

References

Armand S, Vieille C, Gey C, Heyraud A, Zeikus JG, Henrissat B (1996) Stereochemical course and reaction products of the action of β-xylosidase from *Thermoanaerobacterium saccharolyticum* strain B6A-RI. Eur J Biochem 236:706–713

Barkholt V, Jensen AL (1989) Amino acid analysis: determination of cysteine plus half-cystine in proteins after hydrochloric acid hydrolysis with a disulfide compound as additive. Anal Biochem 177:318–322

Britton H, Robinson R (1931) Universal buffer solutions and the association constant of veronal. J Chem Soc 1931:1456–1462

Brunzelle JS, Jordan DB, McCaslin DR, Olczak A, Wawrzak Z (2008) Structure of the two-subsite β-D-xylosidase from *Selenomonas ruminantium* in complex with 1,3-bis[tris(hydroxymethyl)methylamino]propane. Arch Biochem Biophys 474:157–166

Brüx C, Ben-David A, Shallom-Shezifi D, Leon M, Niefind K, Shoham G, Shoham Y, Schomburg D (2006) The structure of an inverting GH43 β-xylosidase from *Geobacillus stearothermophilus* with its substrate reveals the role of the three catalytic residues. J Mol Biol 359:97–109

Cantarel BL, Coutinho PM, Rancurel C, Bernard T, Lombard V, Henrissat B (2009) The Carbohydrate-Active EnZymes database (CAZy): an expert resource for Glycogenomics. Nucleic Acids Res 37:D233–D238

Cartmell A, McKee LS, Pena MJ, Larsbrink J, Brumer H, Kaneko S, Ichinose H, Lewis RJ, Viksø-Nielsen A, Gilbert HJ, Marles-Wright J (2011) The structure and function of an arabinan-specific α-1,2-arabinofuranosidase identified from screening the activities of bacterial GH43 glycoside hydrolases. J Biol Chem 286:15483–15495

de Sanctis D, Inacio JM, Lindley PF, de Sa-Nogueira I, Bento I (2010) New evidence for the role of calcium in the glycosidase reaction of GH43 arabinanases. FEBS J 277:4562–4574

Ebringerova A (2006) Structural diversity and application potential of hemicelluloses. Macromol Symp 232:1–12

Ferrer M, Ghazi A, Beloqui A, Vieites JM, Lopez-Cortes N, Marin-Navarro J, Nechitaylo TY, Guazzaroni ME, Polaina J, Waliczek A, Chernikova TN, Reva ON, Golyshina OV, Golyshin PN (2012) Functional metagenomics unveils a multifunctional glycosyl hydrolase from the family 43 catalysing the breakdown of plant polymers in the calf rumen. PLoS One 7:e38134

Gilad O, Jacobsen S, Stuer-Lauridsen B, Pedersen MB, Garrigues C, Svensson B (2010) Combined transcriptome and proteome analysis of *Bifidobacterium animalis* subsp. *lactis* BB-12 grown on xylo-oligosaccharides and a model of their utilization. Appl Environ Microbiol 76:7285–7291

Gilad O, Svensson B, Viborg AH, Stuer-Lauridsen B, Jacobsen S (2011) The extracellular proteome of *Bifidobacterium animalis* subsp. *lactis* BB-12 reveals proteins with putative roles in probiotic effects. Proteomics 11:2503–2514

Gilad O, Hjernø K, Østerlund EC, Margolles A, Svensson B, Stuer-Lauridsen B, Møller AL, Jacobsen S (2012) Insights into physiological traits of *Bifidobacterium animalis* subsp. *lactis* BB-12 through membrane proteome analysis. J Proteomics 75:1190–1200

Gouet P, Courcelle E, Stuart DI, Metoz F (1999) ESPript: analysis of multiple sequence alignments in PostScript. Bioinformatics 15:305–308

Goujon M, McWilliam H, Li W, Valentin F, Squizzato S, Paern J, Lopez R (2010) A new bioinformatics analysis tools framework at EMBL-EBI. Nucleic Acids Res 38:W695–W699

Guerfali M, Gargouri A, Belghith H (2008) Talaromyces thermophilus β-D-xylosidase: purification, characterization and xylobiose synthesis. Appl Biochem Biotechnol 150:267–279

Huson DH, Richter DC, Rausch C, Dezulian T, Franz M, Rupp R (2007) Dendroscope: An interactive viewer for large phylogenetic trees. BMC Bioinforma 8:460

Jordan DB, Li XL, Dunlap CA, Whitehead TR, Cotta MA (2007) β-D-xylosidase from Selenomonas ruminantium of glycoside hydrolase family 43. Appl Biochem Biotechnol 137–140:93–104

Kim YA, Yoon K (2010) Characterization of a Paenibacillus woosongensis β-xylosidase/α-arabinofuranosidase produced by recombinant Escherichia coli. J Microbiol Biotechnol 20:1711–1716

Lagaert S, Pollet A, Delcour JA, Lavigne R, Courtin CM, Volckaert G (2011) Characterization of two β-xylosidases from Bifidobacterium adolescentis and their contribution to the hydrolysis of prebiotic xylooligosaccharides. Appl Microbiol Biotechnol 92:1179–1185

Macfarlane S, Macfarlane GT, Cummings JH (2006) Review article: prebiotics in the gastrointestinal tract. Aliment Pharmacol Ther 24:701–714

Mai V, Wiegel J, Lorenz WW (2000) Cloning, sequencing, and characterization of the bifunctional xylosidase-arabinosidase from the anaerobic thermophile Thermoanaerobacter ethanolicus. Gene 247:137–143

Makarova K, Slesarev A, Wolf Y, Sorokin A, Mirkin B, Koonin E, Pavlov A, Pavlova N, Karamychev V, Polouchine N, Shakhova V, Grigoriev I, Lou Y, Rohksar D, Lucas S, Huang K, Goodstein DM, Hawkins T, Plengvidhya V, Welker D, Hughes J, Goh Y, Benson A, Baldwin K, Lee JH, Diaz-Muniz I, Dosti B, Smeianov V, Wechter W, Barabote R, Lorca G, Altermann E, Barrangou R, Ganesan B, Xie Y, Rawsthorne H, Tamir D, Parker C, Breidt F, Broadbent J, Hutkins R, O'Sullivan D, Steele J, Unlu G, Saier M, Klaenhammer T, Richardson P, Kozyavkin S, Weimer B, Mills D (2006) Comparative genomics of the lactic acid bacteria. Proc Natl Acad Sci U S A 103:15611–15616

Mäkeläinen H, Forssten S, Saarinen M, Stowell J, Rautonen N, Ouwehand AC (2010) Xylo-oligosaccharides enhance the growth of bifidobacteria and Bifidobacterium lactis in a simulated colon model. Benef Microbes 1:81–91

Miller GL (1959) Use of dinitrosalicylic acid reagent for determination of reducing sugar. Anal Chem 31:426–428

Minic Z, Rihouey C, Do CT, Lerouge P, Jouanin L (2004) Purification and characterization of enzymes exhibiting β-D-xylosidase activities in stem tissues of Arabidopsis. Plant Physiol 135:867–878

Moure A, Gullon P, Dominguez H, Parajo JC (2006) Advances in the manufacture, purification and applications of xylo-oligosaccharides as food additives and nutraceuticals. Process Biochem 41:1913–1923

Nurizzo D, Turkenburg JP, Charnock SJ, Roberts SM, Dodson EJ, McKie VA, Taylor EJ, Gilbert HJ, Davies GJ (2002) Cellvibrio japonicus α-L-arabinanase 43A has a novel five-blade β-propeller fold. Nat Struct Biol 9:665–668

Pitson SM, Voragen AG, Beldman G (1996) Stereochemical course of hydrolysis catalyzed by arabinofuranosyl hydrolases. FEBS Lett 398:7–11

Qian Y, Yomano LP, Preston JF, Aldrich HC, Ingram LO (2003) Cloning, characterization, and functional expression of the Klebsiella oxytoca xylodextrin utilization operon (xynTB) in Escherichia coli. Appl Environ Microbiol 69:5957–5967

Ravanal MC, Callegari E, Eyzaguirre J (2010) Novel bifunctional α-L-arabinofuranosidase/xylobiohydrolase (ABF3) from Penicillium purpurogenum. Appl Environ Microbiol 76:5247–5253

Roberfroid M (2007) Prebiotics: the concept revisited. J Nutr 137:830S–837S

Ruas-Madiedo P, Hernandez-Barranco A, Margolles A, de los Reyes-Gavilan CG (2005) A bile salt-resistant derivative of Bifidobacterium animalis has an altered fermentation pattern when grown on glucose and maltose. Appl Environ Microbiol 71:6564–6570

Rycroft CE, Jones MR, Gibson GR, Rastall RA (2001) A comparative in vitro evaluation of the fermentation properties of prebiotic oligosaccharides. J Appl Microbiol 91:878–887

Sakka K, Yoshikawa K, Kojima Y, Karita S, Ohmiya K, Shimada K (1993) Nucleotide sequence of the Clostridium stercorarium xylA gene encoding a bifunctional protein with β-D-xylosidase and α-L-arabinofuranosidase activities, and properties of the translated product. Biosci Biotechnol Biochem 57:268–272

Shallom D, Leon M, Bravman T, Ben-David A, Zaide G, Belakhov V, Shoham G, Schomburg D, Baasov T, Shoham Y (2005) Biochemical characterization and identification of the catalytic residues of a family 43 β-D-xylosidase from Geobacillus stearothermophilus T-6. Biochemistry 44:387–397

Söding J, Biegert A, Lupas AN (2005) The HHpred interactive server for protein homology detection and structure prediction. Nucleic Acids Res 33:W244–W248

Suryani KT, Sakka K, Ohmiya K (2004) Sequencing and expression of the gene encoding the Clostridium stercorarium β-xylosidase Xyl43B in Escherichia coli. Biosci Biotechnol Biochem 68:609–614

Tenkanen M, Luonteri E, Teleman A (1996) Effect of side groups on the action of β-xylosidase from Trichoderma reesei against substituted xylo-oligosaccharides. FEBS Lett 399:303–306

Utt EA, Eddy CK, Keshav KF, Ingram LO (1991) Sequencing and expression of the Butyrivibrio fibrisolvens xylB gene encoding a novel bifunctional protein with β-D-xylosidase and α-L-arabinofuranosidase activities. Appl Environ Microbiol 57:1227–1234

van den Broek LAM, Hinz SWA, Beldman G, Vincken J, Voragen AGJ (2008) Bifidobacterium carbohydrases-their role in breakdown and synthesis of (potential) prebiotics. Mol Nutr Food Res 52:146–163

Vandermarliere E, Bourgois TM, Winn MD, van Campenhout S, Volckaert G, Delcour JA, Strelkov SV, Rabijns A, Courtin CM (2009) Structural analysis of a glycoside hydrolase family 43 arabinoxylan arabinofuranohydrolase in complex with xylotetraose reveals a different binding mechanism compared with other members of the same family. Biochem J 418:39–47

Wagschal K, Franqui-Espiet D, Lee CC, Kibblewhite-Accinelli RE, Robertson GH, Wong DWS (2007) Genetic and biochemical characterization of an α-L-arabinofuranosidase isolated from a compost starter mixture. Enzyme Microb Technol 40:747–753

Wagschal K, Heng C, Lee CC, Wong DW (2009a) Biochemical characterization of a novel dual-function arabinofuranosidase/xylosidase isolated from a compost starter mixture. Appl Microbiol Biotechnol 81:855–863

Wagschal K, Heng C, Lee CC, Robertson GH, Orts WJ, Wong DW (2009b) Purification and characterization of a glycoside hydrolase family 43 β-xylosidase from Geobacillus thermoleovorans IT-08. Appl Biochem Biotechnol 155:304–313

Whitehead TR, Cotta MA (2001) Identification of a broad-specificity xylosidase/arabinosidase important for xylooligosaccharide fermentation by the ruminal anaerobe Selenomonas ruminantium GA192. Curr Microbiol 43:293–298

Xiong JS, Balland-Vanney M, Xie ZP, Schultze M, Kondorosi A, Kondorosi E, Staehelin C (2007) Molecular cloning of a bifunctional β-xylosidase/α-L-arabinosidase from alfalfa roots: heterologous expression in Medicago truncatula and substrate specificity of the purified enzyme. J Exp Bot 58:2799–2810

Xu WZ, Shima Y, Negoro S, Urabe I (1991) Sequence and properties of β-xylosidase from Bacillus pumilus IPO. Contradiction of the previous nucleotide sequence. Eur J Biochem 202:1197–1203

Zhou J, Bao L, Chang L, Zhou Y, Lu H (2012) Biochemical and kinetic characterization of GH43 β-D-xylosidase/α-L-arabinofuranosidase and GH30 α-L-arabinofuranosidase/β-D-xylosidase from rumen metagenome. J Ind Microbiol Biotechnol 39:143–152